

Mössbauer-Effect Studies of Iron-Tin Alloys

Trumpy, Georg; Both, Erik; Djéga-Mariadassou, C.; Lecocq, P.

Published in:
Physical Review B (Condensed Matter and Materials Physics)

Link to article, DOI:
[10.1103/PhysRevB.2.3477](https://doi.org/10.1103/PhysRevB.2.3477)

Publication date:
1970

Document Version
Publisher's PDF, also known as Version of record

[Link back to DTU Orbit](#)

Citation (APA):
Trumpy, G., Both, E., Djéga-Mariadassou, C., & Lecocq, P. (1970). Mössbauer-Effect Studies of Iron-Tin Alloys. *Physical Review B (Condensed Matter and Materials Physics)*, 2(9), 3477-3490. DOI: 10.1103/PhysRevB.2.3477

DTU Library

Technical Information Center of Denmark

General rights

Copyright and moral rights for the publications made accessible in the public portal are retained by the authors and/or other copyright owners and it is a condition of accessing publications that users recognise and abide by the legal requirements associated with these rights.

- Users may download and print one copy of any publication from the public portal for the purpose of private study or research.
- You may not further distribute the material or use it for any profit-making activity or commercial gain
- You may freely distribute the URL identifying the publication in the public portal

If you believe that this document breaches copyright please contact us providing details, and we will remove access to the work immediately and investigate your claim.

21, 1589 (1968).

⁶J. Tylicki, W. M. Yen, J. P. van der Ziel, and H. J. Guggenheim, *Phys. Rev.* **187**, 758 (1969).

⁷P. A. Fleury, J. M. Worlock, and H. J. Guggenheim, *Phys. Rev.* **185**, 738 (1969).

⁸M. P. Petrov, V. V. Moskalev, and G. A. Smolenskii, *Solid State Commun.* **8**, 157 (1970).

⁹E. I. Golovenchits, V. A. Sanina, and A. G. Gurevich, *Fiz. Tverd. Tela* **10**, 2956 (1968) [*Soviet Phys. Solid State* **10**, 2334 (1969)].

¹⁰M. P. Petrov and S. A. Kizhaev, *Fiz. Tverd. Tela* **11**, 2435 (1969) [*Soviet Phys. Solid State* **11**, 1968 (1970)].

¹⁴G. A. Smolenskii, M. P. Petrov, V. V. Moskalev,

V. S. L'vov, V. S. Kasperovich, and E. V. Zhirnova, *Fiz. Tverd. Tela* **10**, 1305 (1968) [*Soviet Phys. Solid State* **10**, 1040 (1968)].

¹²P. R. Locher and S. Geschwind, *Phys. Rev. Letters* **11**, 333 (1963).

¹³A. Abragam and M. H. L. Pryce, *Proc. Roy. Soc. (London)* **A205**, 135 (1951).

¹⁴A. J. Freeman and R. E. Watson, in *Magnetism IIA*, edited by G. T. Rado and H. Suhl (Academic, New York, 1965), p. 167.

¹⁵W. J. Childs and L. S. Goodman, *Phys. Rev.* **170**, 136 (1968).

¹⁶R. M. Sternheimer, *Phys. Rev.* **146**, 140 (1966).

Mössbauer-Effect Studies of Iron-Tin Alloys

G. Trumpy and E. Both

Laboratory of Applied Physics II, Technical University of Denmark, Lyngby, Denmark

and

C. Djéga-Mariadassou and P. Lecocq

Laboratoire de Chimie Minérale, Faculté des Sciences, Orsay, France

(Received 16 March 1970)

Solid solutions $FeSn$ and the compounds Fe_3Sn , Fe_5Sn_3 , Fe_3Sn_2 , $FeSn$, and $FeSn_2$ have been studied by the Mössbauer effect in both Fe and Sn nuclei. Also, standard x-ray diffraction and magnetization studies were performed. The magnetic hyperfine (hf) fields in the Fe and Sn components are not, in general, proportional to the magnetic moments. It is found that two simple relations containing the coordination numbers can be used within a wide range to describe the variations of these fields as a function of composition. The collected results indicate that the magnetic hf field at the iron nucleus is rather insensitive to the conduction-electron polarization in these alloys. The isomer shifts are linearly related to the number of Fe-Sn bonds in such a way that bonding reduces the electron densities at both nuclei. The bonding is covalentlike and predominantly unpolarized.

I. INTRODUCTION

The origins of the hyperfine (hf) effects in metals and alloys are, at present, only poorly understood. This is partly due to the fact that one has still not a satisfactory description of electrons in alloys or of ordered magnetic phenomena in metals and alloys. These problems may be approached through systematic experimental studies of hf effects, which, for instance, can be observed as a function of sample composition.

In the present work, we have carried out a study of hf structure, measured by means of the Mössbauer effect, on all the known different phases of the binary iron-tin alloy system. Both of these two components are in practice very useful Mössbauer nuclei in a wide temperature range, this being part of the reason for choosing such a system. Data on the alloys were also obtained by means of more conventional methods, such as magnetic-moment and Curie-point determinations and x-ray crystallog-

raphy. The experimental results do in fact show certain regularities which may prove to be of some value in formulating theories on hf effects and in planning future experiments. It appears that hf magnetic fields and electron densities may be expressed as simple functions of the atom's surroundings. Some general relationships will tentatively be proposed and the physical mechanisms will be discussed.

II. EXPERIMENTAL METHODS

The known phases of the iron-tin system have been given by Hansen and Anderko,¹ and by Jannin *et al.*² The phase diagram is characterized by one solid solution, $FeSn$, and five definite intermetallic compounds, Fe_3Sn , Fe_5Sn_3 , Fe_3Sn_2 , $FeSn$, and $FeSn_2$.

Polycrystalline samples were prepared by diffusion. Known quantities of 99.9+% tin powder and 99.9+% iron powder contained in an evacuated quartz ampoule were annealed for fifteen days at the equilibrium temperature of the relevant phase. The samples of Fe_5Sn_3 were annealed for one month. Fin-

ally, the ampoule was quenched in water. Crystal structure and sample purity were studied by means of conventional x-ray-powder spectrometry and spectroscopy.

The Mössbauer spectrometers used were of conventional design. The source was usually placed on an electromagnetic transducer moving with constant acceleration. Data were recorded on a 512-channel pulse-height analyzer operating in amplitude mode. In a few special cases, when parts of the spectra should be studied, a constant velocity spectrometer was employed. The sources were Co^{57} in Pd and Sn^{119} in Mg_2Sn , at room temperature. Absorbers, consisting of finely ground powders placed between plastic or mica sheets, could be heated or cooled. Provision was made for the absorbers to be placed in an external magnetic field of 10 or 17 kG applied either along or across the γ -emission direction being studied. The absorption-spectrum linewidth ranged from 0.29 to 0.34 mm/sec in "good" spectra (Fe_3Sn , Fe_3Sn_2 , FeSn_2 , and FeSn) for the 14-keV radiation of Co^{57} , and it was 1.1 mm/sec for the 24-keV radiation of Sn^{119} (Fe_3Sn).

The saturation magnetization of the alloys was obtained by the Weiss-Forrer method. The sample, being cooled to liquid-nitrogen temperature, was quickly brought into a region of a strong homogeneous field where the magnetic induction caused by the sample was recorded by a couple of test coils connected to a ballistic galvanometer. Curie-point determinations were performed by recording the force upon the sample placed in an inhomogeneous magnetic field as a function of sample temperature.

III. RESULTS AND SPECIAL STRUCTURES

The more important data obtained by Mössbauer-effect and by magnetic-moment studies are presented in Table I. In particular, Fig. 1 shows a graphic representation of the magnetic hf fields $H_{\text{eff}}(\text{Fe})$ and $H_{\text{eff}}(\text{Sn})$ observed at the respective nuclei and the average magnetic moment $\bar{\mu}_{\text{Fe}}$, which for the ferromagnets is given by the saturation magnetization divided by the number of iron atoms, and for the antiferromagnets it is the moment obtained by neutron diffraction.³⁻⁵ Figure 2 shows the value of $H_{\text{eff}}(\text{Sn})/\bar{\mu}_{\text{Fe}}$ as a function of aligned Fe-atom coordination N_{SnFe^+} . The reason for this representation is discussed in Sec. VI.

For the ferromagnetic compounds Fe_3Sn , Fe_5Sn_3 , and Fe_3Sn_2 , the direction of the hf magnetic field was found to be opposite to the external magnetization in both iron and tin positions. Also, the effect of an external magnetic field upon the Fe^{57} Mössbauer spectra is clearly a proportional contraction of all line positions. In this way, it is established that all these compounds are ferro- and not ferrimagnetic.

Goodenough⁶ has worked out a theory for the magnetism of binary compounds based upon the magnetic

TABLE I. Experimental results for Fe-Sn alloys at 77°K.

Compound	Magn. order ^a	Trans. temp. (°C)	$\bar{\mu}_{\text{Fe}}$ (μ_B)	Fe site	Intensity (%)	$H_{\text{eff}}(\text{Fe})$ (kG)	δ_{Fe} (mm/sec)	ϵ_{Fe} (mm/sec)	Sn site	Intensity (%)	$H_{\text{eff}}(\text{Sn})$ (kG)	ϵ_{Sn} (mm/sec)	ϵ_{Sn} (mm/sec)
Fe	F	765	2.218			-338	0(def.)						
FeSn 4 at. % Sn	F			0 nn Sn	72	-338 ± 3	0.03 ± 0.02	0.00 ± 0.02			66 ± 6	-1.2 ± 0.2	...
				1 nn Sn	24	-320 ± 3	0.11 ± 0.03	-0.03 ± 0.03					
				2 nn Sn	4	-303 ± 5	0.12 ± 0.07	-0.08 ± 0.07					
FeSn 8 at. % Sn	F	760		0 nn Sn	51	-343 ± 3	0.04 ± 0.02	0.01 ± 0.02			59 ± 4	-1.2 ± 0.1	...
				1 nn Sn	36	-321 ± 3	0.13 ± 0.03	0.02 ± 0.03					
				2 nn Sn	11	-298 ± 5	0.20 ± 0.07	-0.03 ± 0.07					
Fe_3Sn	F	470	2.27 ± 0.02			-268 ± 2	0.53 ± 0.02	0.06 ± 0.02		103 ± 2	-0.86 ± 0.04	0.02 ± 0.04	
Fe_5Sn_3 (840°C)	F	315		Fe'	54 ± 7	-204 ± 4	0.64 ± 0.06	0.09 ± 0.06	Several sites		74 ± 6	-1.0 ± 0.1	...
				Fe''	36 ± 7	-195 ± 5	0.53 ± 0.06	-0.02 ± 0.06					
				Fe'''	10 ± 5	-255 ± 15	...						
Fe_3Sn_2	F	339		Fe I	67 ± 5	-219 ± 2	0.59 ± 0.02	0.06 ± 0.02	Several sites		From 0 to 73 ± 2	-0.49 ± 0.06	...
				Fe II	33 ± 5	-211 ± 3	0.54 ± 0.02	-0.02 ± 0.03					
FeSn	A	95	1.7 ± 0.1 ^b	Fe I	67 ± 5	167 ± 2	0.65 ± 0.02	0.00 ± 0.02	Sn I	67 ± 3	0 ^b	-0.57 ± 0.04	0.74 ± 0.04
				Fe II	33 ± 5	139 ± 2	0.59 ± 0.02	-0.17 ± 0.02	Sn II	33 ± 3	49 ± 1	-0.39 ± 0.08	0.26 ± 0.08
FeSn_2	A	107	1.6 ± 0.1 ^c			152 ± 2	0.73 ± 0.03	0.02 ± 0.03		33 ± 2	-0.32 ± 0.05	0.15 ± 0.05	

^aF is for ferromagnetic and A is for antiferromagnetic.

^bSee Refs. 3 and 4.

^cSee Ref. 5.

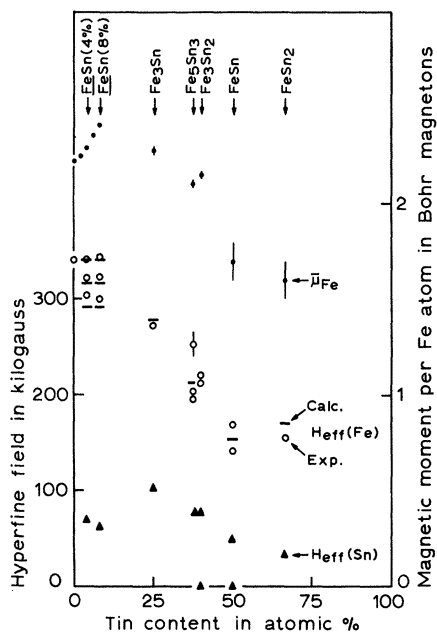


FIG. 1. Magnetic moment per Fe atom in the known iron-tin alloys (black dots), and the magnetic hf fields at Fe (circles) and Sn (triangles) positions. Short horizontal bars are average values of $H_{\text{eff}}(\text{Fe})$ as given by Eq. (3).

properties of interatomic bonding. For the case of Fe_xSn , he predicts that the compound is purely ferromagnetic for $x > 1.7$, and it may contain some ferromagnetic regions in the vicinity of $x = 1.5$, provided that it has the NiAs structure. We actually find ferromagnetism for $x > 1.5$. It should be noted that Fe_3Sn_3 ($x = 1.67$) has NiAs structure, but Fe_3Sn_2 has not.

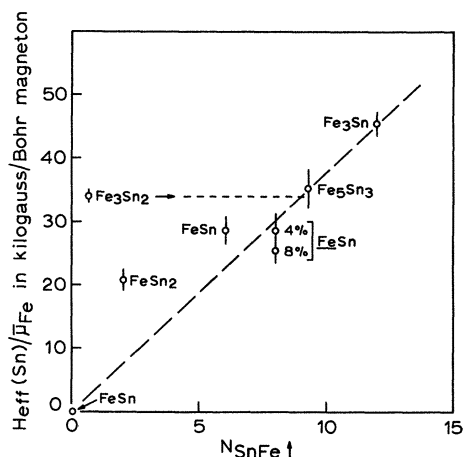


FIG. 2. Ratio of magnetic hf field at Sn sites to the magnetic moment per Fe atom in iron-tin alloys. The inclined dashed line is given by Eq. (7).

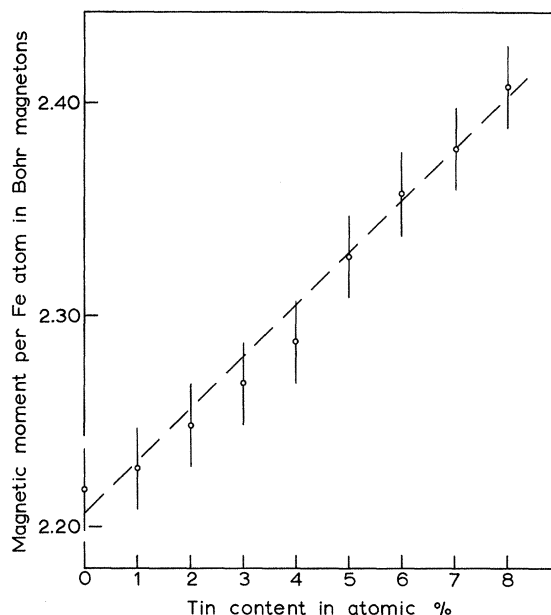


FIG. 3. Magnetic moment per Fe atom in the solid solutions FeSn .

A. FeSn

Solid solutions of tin in iron were prepared by diffusion at temperatures between 900 and 1100 °C. X-ray studies were performed on samples with atomic tin content between 1 and 9%. We find that the limiting solubility of tin in iron is 8.5 at. % at 1070 °C. The lattice constant in the bcc structure increases from $a = 2.867 \text{ \AA}$ in iron to $a = 2.920 \text{ \AA}$ at 9-at. % tin content.

The saturation magnetic moment was measured for alloys with up to 8-at. % tin, and the results are given in Fig. 3. Our own results are in reasonable agreement with earlier measurements by Fallo⁷ and Aldred⁸ although our data show a stronger dependence upon tin content. The straight line drawn through the value for iron metal implies that the alloy is a primary solid solution, meaning that the tin atoms interact little or not at all with each other.

The Mössbauer spectra for the iron nuclei in FeSn consist of several superimposed six-line spectra caused by 0, 1, and 2 nearest-neighbor solute atoms, as is generally the case for substitutional alloys.^{9,10} The data obtained for $H_{\text{eff}}(\text{Fe})$, as shown in Table I, are compatible with the empirical formula for FeSn given by Wertheim *et al.*⁹ The tin spectrum is strongly smeared out, but the average magnetic field is clearly found to be numerically smaller than the value of -81 kG reported earlier.¹¹

B. Fe_3Sn

This compound is stable between 750 and 850 °C,¹ and was produced by diffusion at 800 °C. X-ray cry-

stallography on different compositions shows that this phase is obtained in its purest form in an alloy containing 24.5-at.% tin. It is ferromagnetic with the Curie point $\tau_c = 470^\circ\text{C}$. The structure is DO_{19} as established by Nial,¹² with $a = 5.458 \text{ \AA}$, $c = 4.361 \text{ \AA}$, and otherwise as given in Table II. The coordinations used for the application of Eqs. (3) and (7) were chosen as if the two interatomic distances 2.73 and 2.69 \AA were equal.

Mössbauer spectra with both iron and tin sources are clearly resolved into six narrow single lines, showing that there is only one kind of magnetic hf field for each type of nucleus. A natural conclusion is that the field is directed along the c axis, since any other magnetization direction would include more than one combination of magnetic field and EFG tensor for each sublattice.

One Fe^{57} Mössbauer spectrum was taken at 800°C , where the absorber is stable and paramagnetic. The quadrupole splitting was $2\epsilon = 0.16 \pm 0.01 \text{ mm/sec}$, in fair agreement with the value obtained from the displacement of the Zeeman lines in the ferromagnetic state. This shows that the EFG tensor has its major axis along, or nearly along, the magnetic-moment direction. Attempts to measure between 200 and 750°C were not successful, as the absorber was then slowly decomposing.

C. Fe_5Sn_3

This phase is stable between 780 and 900°C .¹³ Samples were prepared by diffusion for one month at the desired temperature. X-ray-powder diagrams taken on "high-temperature" (900°C) and "low-temperature" (840°C) samples show that these two modifications have different structures. They both appear to have the hexagonal structure of space group D_6^4h , but with different lattice parameters and line

TABLE II. Structure and coordinations for $\text{Fe}_3\text{Sn}(\text{Fe}_6\text{Sn}_2)$

Atom	Number in unit cell	Positions in cell	Nearest neighbors	Distances (\AA)
Fe	6	$\frac{1}{3} \frac{1}{6} \frac{1}{4}$	4 Fe	2, 73
		$\frac{5}{6} \frac{1}{6} \frac{1}{4}$		
		$\frac{5}{6} \frac{2}{3} \frac{1}{4}$		
		$\frac{2}{3} \frac{5}{6} \frac{3}{4}$		
		$\frac{1}{6} \frac{5}{6} \frac{3}{4}$		
		$\frac{1}{6} \frac{1}{3} \frac{3}{4}$		
Sn	2	$\frac{1}{3} \frac{2}{3} \frac{1}{4}$	6 Fe	2, 73
		$\frac{2}{3} \frac{1}{3} \frac{3}{4}$		

TABLE III. Experimental results for the two phases of Fe_5Sn_3 .

Formation temp. ($^\circ\text{C}$)	Lattice parameters (\AA)		Curie temp. ($^\circ\text{C}$)	$H_{\text{eff}}(\text{Fe})$ (kG)	Rel. int. (%)	$H_{\text{eff}}(\text{Sn})$ (kG)
	a	c				
840	4.217($\times 4$)	5.245	315 \pm 3	-204 \pm 4	54 \pm 7	74 \pm 6
				-195 \pm 5	36 \pm 7	
				-255 \pm 15	10 \pm 5	
900	4.230	5.208	359 \pm 3	(204)	37 \pm 5	25 \pm 5
				(-195)	38 \pm 5	
				(-255)	25 \pm 5	

intensities. We also find that the Curie temperature is different in the two cases. These data are given in Table III. In Table IV, we give the structure for Fe_5Sn_3 (900°C) as obtained by x-ray-powder-diagram analysis. This can be considered as the NiAs structure, where two-thirds of the trigonal-bipyramidal holes formed by tin atoms have been occupied by Fe II interstitials, and one-third of these holes are vacant.⁶ In the 900°C compound, these vacancies are randomly distributed, while the 840°C compound has a superstructure with basis length $4a$, indicating the onset of ordering as the temperature is lowered. A detailed study of this structure is in progress, and will be published elsewhere.¹³

The Mössbauer spectra obtained for the Fe_5Sn_3 compounds all have quite broad lines (see Fig. 4) indicating that each sample contains some disorder or local inhomogeneities. Fe^{57} spectra taken in external fields show that ferrimagnetism must be excluded in both phases. The separation into three components with different $H_{\text{eff}}(\text{Fe})$, as given in Table III, is obtained after a study of several spectra taken at different temperatures. The Mössbauer spectrum for Sn¹¹⁹ is strongly smeared out, and is obviously resulting from several tin sites with dif-

TABLE IV. Proposed structure and coordinations for Fe_5Sn_3 ($\text{Fe}_{10}\text{Sn}_6$) at 900°C .

Atom	No. in unit cell	Positions in cell	Nearest neighbors	Distances (\AA)
Fe I	6	$0 \ 0 \ 0$	2 Fe I 6 Sn	2.60 2.77
		$0 \ 0 \ \frac{1}{2}$		
		$\frac{1}{3} \ \frac{2}{3} \ \frac{3}{4}$		
		$\frac{2}{3} \ \frac{1}{3} \ \frac{1}{4}$		
		$\frac{1}{3} \ \frac{2}{3} \ \frac{1}{4}$		
		$\frac{2}{3} \ \frac{1}{3} \ \frac{3}{4}$		
Fe II	4	$\frac{1}{3} \ \frac{2}{3} \ \frac{3}{4}$	6 Fe I 3 Sn	2.77 2.44
		$\frac{2}{3} \ \frac{1}{3} \ \frac{1}{4}$		
Sn	6	$\frac{1}{3} \ \frac{2}{3} \ \frac{1}{4}$	6 Fe I 0-5 Fe II	2.60 2.77
		$\frac{2}{3} \ \frac{1}{3} \ \frac{3}{4}$		

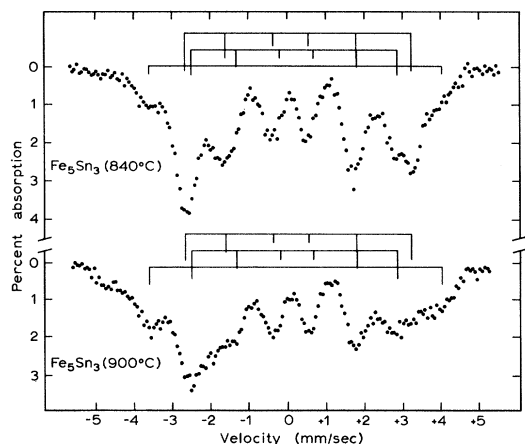


FIG. 4. Fe^{57} Mössbauer spectra at 300 °K for the high- and low-temperature modifications of Fe_5Sn_3 . The subdivision into three separate components was decided on the basis of several spectra obtained at different temperatures.

ferent properties. Only an average $H_{\text{eff}}(\text{Sn})$ can be obtained.

Both modifications of Fe_5Sn_3 have the field $H_{\text{eff}}(\text{Fe}) = 195$ kG, with roughly 40% intensity. This can be ascribed to the Fe II atoms which all have a coordination of 6 Fe I. The rest of the Mössbauer spectrum for 900 °C is strongly smeared out, which could agree with Fe I contributions having Fe coordinations varying between 8 and 2 as shown in Table IV. The increased order at lower formation temperature is reflected by a simpler Fe^{57} Mössbauer spectrum for Fe_5Sn_3 (840 °C). It appears that the high-field component is less intense, and most of the Fe I atoms (about five per unit cell) probably have a coordination of 3 or 4 Fe II.

As the variations in H_{eff} from one site to another are caused by local variations in the electron spin distribution, they cannot be predicted by the simple Eqs. (3) and (7) of Secs. IV and VI. In Eq. (3), we have inserted the average coordination numbers $\bar{N}_{\text{FeFe}} = 5.83$ and $\bar{N}_{\text{FeSn}} = 5.6$, based upon the values in Table IV. This gives the result $H_{\text{eff}}(\text{Fe}) = 206$ kG, which coincides accurately with the observed average, as obtained from the values in Table I. The average $\bar{N}_{\text{SnFe}} = 9.3$ was used for plotting Fe_5Sn_3 in Fig. 2.

Previously, Yamamoto¹⁴ made x-ray and Mössbauer-effect studies of this compound, also finding two different structures. Some of the details in his interpretation are at variance with ours. We do not know the reason for these discrepancies, but part of the cause can be that his quenching temperatures were different from ours.

D. Fe_3Sn_2

This compound is stable between 600 and 815 °C, and it was prepared by diffusion at 700 °C. We

have not been able to interpret the complex x-ray-powder diagrams obtained from this substance. Nial¹² reports that the unit cell contains 40 atoms = 8 Fe_3Sn_2 . It is monoclinic, $a = 13.53$ Å, $b = 5.34$ Å, $c = 9.20$ Å, and $\beta = 103^\circ$, but the detailed structure has not been resolved. The Curie temperature is $\tau_c = 339$ °C.

The Fe^{57} Mössbauer spectrum shows one field, $H_{\text{eff}}(\text{Fe}) = (199 \pm 2)$ kG, at room temperature and two fields, $H_{\text{eff}}(\text{Fe}) = (219 \pm 2)$ kG and (211 ± 2) kG with intensity ratio 2:1, at liquid-nitrogen temperature. We have found that there exists a transition temperature $\tau_1 = (114 \pm 3)$ °K at which the two fields merge into one. This temperature is strongly field dependent, as application of an external magnetic field of 4 kG at room temperature causes a transition from the one-field case to the two-field case.

The Sn^{119} Mössbauer spectrum has not been resolved. Probably there are about four different $H_{\text{eff}}(\text{Sn})$. There is a marked difference between the spectra at room temperature and at liquid-nitrogen temperature.

Since the structure is unknown, the coordination-dependent equations (3), (7), (9), and (10) can not be checked by the observed hf effects in Fe_3Sn_2 . On the other hand, if the equations are considered to express reliable empirical laws, information on the structure can be obtained by use of the hf field data. From Fig. 2, which is discussed below, one sees that the observed maximum $H_{\text{eff}}(\text{Sn})$ is consistent with $N_{\text{SnFe}} = 9.0 \pm 0.5$, which should be the case for about 20% of the tin atoms. The rest of the rather smeared-out Mössbauer spectrum indicates that $N_{\text{FeSn}} \leq 2$ for 80% of the Sn atoms. The coordination N_{FeSn} to be used in Eq. (3) is given by the bonds that have a strength comparable to the Fe-Fe bonds. From the above result, we can only deduce a maximum for the average: $\bar{N}_{\text{FeSn}} \leq \frac{2}{3} \bar{N}_{\text{SnFe}} \approx 2$. The observed $H_{\text{eff}}(\text{Fe}) = 220$ kG is then obtained if the corresponding value $\bar{N}_{\text{FeFe}} = 5$ is chosen.

The regularities among the isomer-shift data are best satisfied if we choose the following numbers for conduction-electron bonding (which need not be the same as the coordinations used in the equations for H_{eff}): $N_{\text{SnFe}} \approx 7.5$ and $N_{\text{FeSn}} \approx 5.0$.

One might conclude that the iron coordination is about 5 Fe and 5 Sn, but only one or two of the latter atoms are so close that they influence the magnetic structure. The tin coordination is 8 ± 1 Fe, but only in 20% of the cases is the Sn-Fe distance short enough to produce a transferred magnetic field.

E. FeSn

This compound is stable up to 740 °C.¹ It was formed by diffusion at 450 °C. It is known that this phase is not ferromagnetic, and it has the hexagonal

structure of the B-35 type ($a = 5.300 \text{ \AA}$, $c = 4.449 \text{ \AA}$),^{2,12} as given in Table V. The magnetic structure has been analyzed by neutron-diffraction measurements,^{3,4} which show that the iron atoms are ordered ferromagnetically in planes $z = \text{constant}$, and with opposite magnetization directions for $z = 0, 2c, 4c, \dots$ and for $z = c, 3c, \dots$.

Previous Mössbauer-effect measurements^{14,15} show that the Néel temperature is $(95 \pm 2) \text{ }^\circ\text{C}$. Our present spectrum for Fe^{57} has improved resolution, and it is interpreted as a superposition of two six-line spectra in the ratio 2:1 (see Fig. 5). Two magnetically different iron sites with this intensity ratio will result if the magnetic-moment vectors are lying in the ferromagnetic planes, either along the Sn-Fe-Sn direction, the x axis, or perpendicular to this direction. If we assume an axially symmetric EFG tensor along the x axis, it is easy to calculate the relative quadrupole splits and the form of the spectra for the two sites in both cases. Such a calculation shows unambiguously that the case of H_{eff} parallel to the EFG axis gives the best interpretation of the experimental spectrum. The magnetic fields obtained from this fitting procedure are included in Table I. The highest H_{eff} is found for Fe atoms arranged in chains along the magnetization direction. This shows that H_{eff} depends not only upon coordination number [as in Eq. (3) below], but also upon the coordination geometry.

If the EFG tensor is axially symmetric, and if we assume the Fe quadrupole moment to be $Q = 0.33b$, the field gradient is given by $q = (62 \pm 7) \times 10^{38} \text{ V/m}^2$. Above the Néel point, at $100 \text{ }^\circ\text{C}$, the corresponding magnitude is $q = (95 \pm 8) \times 10^{38} \text{ V/m}^2$. Deviation from EFG axial symmetry is of course possible, since it would hardly be detected in this experiment.

The Sn^{119} Mössbauer spectrum is consistent with this model, since two-thirds of the atoms have $H_{\text{eff}} = 0$, corresponding to the fact that this position has 3 Fe \uparrow and 3 Fe \downarrow neighbors.

F. FeSn_2

This is the most extensively studied Fe-Sn compound. It has the tetragonal CuAl_2 (C16)-type structure (Table VI) with $a = 6.535 \text{ \AA}$, $c = 5.32 \text{ \AA}$,

TABLE V. Structure and coordinations for FeSn (Fe_3Sn_3).

Atom	No. in unit cell	Positions in cell	Nearest neighbors	Distances (\AA)
Fe	3	$\frac{1}{2}$ 0 0	4 Fe \uparrow	2.65
			2 Sn I	2.65
			4 Sn II	2.70
Sn I	1	0 0 0	6 Fe \uparrow	2.65
Sn II	2	$\frac{1}{3}$ $\frac{1}{3}$ $\frac{1}{2}$	3 Sn II	3.06
			6 Fe $\uparrow\downarrow$	2.70

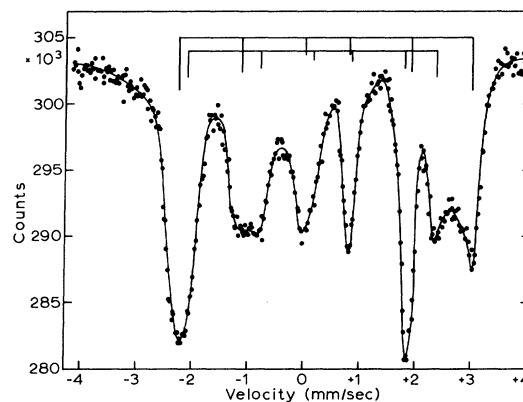


FIG. 5. Fe^{57} Mössbauer spectrum at $77 \text{ }^\circ\text{K}$ for FeSn .

and $x = 0.159$.¹⁶ Neutron-diffraction studies¹⁷ have shown that the Fe atoms are ferromagnetically ordered in straight lines along the fourfold symmetry axis (z axis), while the spin direction is opposite for the four nearest Fe neighbours in the xy plane. The magnetic moment has been given as $\bar{\mu}_{\text{Fe}} = 1.6 \mu_B$.

Mössbauer-effect studies on tin and iron nuclei in FeSn_2 have been performed by Nikolaev *et al.*¹⁸ and by Fabri *et al.*¹⁹ Both groups observed the Néel transition, which lies between 105 and $120 \text{ }^\circ\text{C}$. For our purpose, this compound was prepared by diffusion at $450 \text{ }^\circ\text{C}$. The only additional value of our Mössbauer spectra is narrower lines and a more precise determination of the hf fields, as given in Table I.

The observed magnetic hf field at the Sn nucleus is unexpected, since the four nearest neighbors consist of two Fe atoms with spin up and two with spin down. It must be assumed that the Fe-Sn bonds have an asymmetric arrangement, so that every tin atom is particularly strongly bound to one

TABLE VI. Structure and Coordinations for $\text{FeSn}_2(\text{Fe}_4\text{Sn}_8)$.

Atom	No. in unit cell	Positions in cell	Nearest neighbors	Distances (\AA) for $x = 0.159$
Fe	4	0 0 $\frac{1}{4}$	2 Fe \uparrow	2.66
			8 Sn	2.79
Sn	8	x ($\frac{1}{2} + x$) 0	2 Fe \uparrow	2.79
			2 Fe \downarrow	2.79
			1 Sn	2.94
			2 Sn	3.14

of the ferromagnetic rows of iron atoms. In that case, the maximum value of the coordination N_{SnFe} could be 2. This value has been used in Fig. 2, where it is seen that FeSn_2 does not follow the linear relationship suggested by the ferromagnetic substances.

The hf field at the Fe nucleus is mainly influenced by the two nearest Fe atoms, so that $N_{\text{FeFe}} = 2$. The best-fitting calculated value, as given in Fig. 1, is obtained by neglecting Fe-Sn bonding in this connection, and setting $N_{\text{FeFe}} = N_{\text{Fe},n} = 2$.

In this case it is obvious that the hf fields are more dependent upon the bonding structure than upon the coordination numbers. If the origin of the hf fields were well known, it might be possible to interpret the observed data in terms of the strengths of the Fe-Fe and the Fe-Sn bonds.

IV. MAGNETIC hf FIELD AT IRON NUCLEI

A. General

For iron and for ferromagnetic-iron-based alloys it is generally assumed that the predominant part of the magnetic field at the iron nuclei, $H_{\text{eff}}(\text{Fe})$, is caused by the "Fermi contact interaction" between the magnetic moment of the nucleus and the s -electron spins. This can be expressed as²⁰

$$H_{\text{eff}} \approx H_c = \frac{8}{3} \pi g \mu_0 S \sum_{ns} [|\psi_{ns,+}(0)|^2 - |\psi_{ns,-}(0)|^2], \quad (1)$$

where H_c is the Fermi contact term of the magnetic hf field, μ_0 is the nuclear magneton, g is the gyromagnetic ratio for the nucleus, S is the total spin of the atom, and $\psi_{ns,\pm}(0)$ is the wave function for the ns electrons with spin up (down) at the nuclear site.

The core-electron contribution is given by the sum taken over closed s -electron shells. Watson and Freeman²⁰⁻²² have calculated this quantity for a number of transition-metal ions using exchange polarization in the Hartree-Fock method. This is done by inclusion of the "exchange energy":

$$J_{\text{ex}} = - \sum_i \sum_{j>i} \delta(m_i, m_j) \times \int \int \Phi_i(1) \Phi_j(2) (1/r_{12}) \Phi_i(2) \Phi_j(1) d\tau_1 d\tau_2, \quad (2)$$

where the δ function gives the condition that only exchange interaction between orbitals with common spin contributes to this term.

Generally, one expects proportionality between magnetic moment and hf field in magnetic alloys. This is a natural assumption, as it is clear that core polarization caused by exchange interaction with $3d$ electrons is the main cause of H_{eff} .^{21,22} Proportionality is indeed observed in some cases, e.g., Fe-Al, Fe-Si,²³ and Fe-Rh²⁴ alloys, but in several other instances, this rule is violated. In the particular case of Fe-Sn alloys, it is apparent

from Table I that proportionality is not obeyed. At low tin concentration the magnetic moment increases while H_{eff} in an atom with a specified coordination stays practically constant, and the average H_{eff} does in fact decrease. In general, the hf field shows stronger variations with composition than the magnetic moment. For the four compounds with tin content above 37 at.%, we find a roughly constant ratio $H_{\text{eff}}(\text{Fe})/\bar{\mu}_{\text{Fe}} = 95 \pm 5 \text{ kG}/\mu_B$, where H_{eff} is the average magnetic hf field when more than one value is observed. The more iron-rich alloys have higher values, up to 152 kG/ μ_B for pure iron. Actually, the magnetic moment of the iron atom has roughly the same value for all the ferromagnetic Fe-Sn alloys, and it is obvious that some other physical properties are responsible for the variations in the hf field.

In making a survey over the experimental values obtained for $H_{\text{eff}}(\text{Fe})$ in Fe-Sn compounds, we find that the following relationship is rather nicely satisfied:

$$H_{\text{eff}}(\text{Fe}') = H_1 (N_{\text{Fe}'\text{Fe}} N_{\text{FeFe},g} / N_{\text{Fe},n})^{1/2}, \quad (3)$$

where Fe' is the atom considered, $N_{\text{Fe},n}$ is its coordination number of iron nearest neighbors, $N_{\text{FeFe},g}$ is the Fe-Fe coordination number which is general for the structure (for instance the coordination determining the electron band structure), and $N_{\text{Fe},n}$ is the total number of nearest neighbors to a Fe atom in the alloy. The constant factor was chosen to give the value for iron metal, so that $H_1 = -119.5 \text{ kG}$.

The choice of relevant coordination numbers is unambiguous in all the alloys except Fe_3Sn_2 and FeSn_2 (cf. Sec. III). In Fig. 1, the values calculated in this way are indicated by short horizontal bars. We find that the experimental average $\bar{H}_{\text{eff}}(\text{Fe})$ is quite well reproduced by (3). This shows that in the first approximation it is apparently satisfactory to disregard the magnitude of magnetic moment completely and to ascribe the variations in $H_{\text{eff}}(\text{Fe})$ entirely to different atomic coordinations.

From the extensive calculations by Watson and Freeman,²⁰⁻²² which were compared with a large body of experimental data, it was seen, beyond any doubt, that the most important part of H_{eff} in a first-series transition-element atom is caused by d - s exchange interaction. The spin-dependent part of the exchange integral is shown above as expression (2). This term favors parallel alignment of s - and d -electron spins. The negative magnetic hf field at the nuclear site is thus the result of a compensating distribution of negative polarization, since the total core-electron spin must be zero. Watson and Freeman's calculations were made for atoms in spherically symmetric surroundings and having a constant degree of d -electron polarization.

The experimental examples that were used for comparison with the theory can be supposed to satisfy these conditions. The same authors have also stated that the s -electron spin density at the nucleus would be very sensitive to spatial variations in the polarization of the d electrons. In the general case, a quantitative prediction of hf fields would require detailed calculations of the s - d exchange interaction involving azimuthal variations in the d -electron wave functions. At present the d -electron wave function in ferromagnetic alloys is only poorly known, and in particular, very little can be said about the spin distribution.

In the present work, we are particularly concerned with iron atoms which could have a nonisotropic d -electron spin distribution, since this is likely when the nearest neighbors consist of both iron and tin atoms. For that case, one may expect that a positive d -electron polarization which is concentrated in a smaller region or in more well-defined bonding directions than in metallic iron will leave more space for the negative spin core s electron and cause a numerically smaller spin density at the nucleus. In the iron-tin intermetallic compounds, part of the $3d$ -electron wave function will consist of localized orbits near the Fe-Sn connecting lines, while the Fe-Fe bond will consist of collective (itinerant) d electrons.^{6,25} The bond between a Fe and a Sn atom can be considered as part of a "cation-anion-cation bonding" (Fe-Sn-Fe) which generally favors a spin distribution of antiferromagnetic nature.⁶ Thus, polarization is not energetically favored for the localized $3d$ orbits in these alloys.

With the purpose of justifying our Eq. (3), we will therefore conjecture that in a ferromagnetic alloy with a nontransition-element sublattice, the degree of $3d$ -electron polarization is not constant in space, but is predominantly represented by the electrons of the Fe-Fe bond. First, we consider the case of a given general lattice with a constant total coordination number $N_{Fe,n} = N_{Fe,Fe} + N_{Fe,Sn}$ for each Fe atom. The structure consists of one iron and one tin sublattice, and we presume that there is only one type of iron site and one type of tin site. Then, the sublattice structures are allowed to vary, so that the coordination of each iron atom is changed by a replacement of Fe atoms by Sn atoms. In this case, we find it reasonable to suppose that the contributions to the hf field caused by Fe-Fe bonds are additive, $H_{eff}(Fe) \propto N_{FeFe}$. This is implicit in Eq. (3), when $N_{Fe'Fe} = N_{FeFe,g}$. Second, we assume that compounds with different values of $N_{Fe',n}$ can be compared in the following way. The hf field at the nucleus of atom Fe' would generally be a function of two factors: (i) the number of Fe-Fe bonds between the Fe' and its nearest neighbors, being $N_{Fe'Fe}$, and (ii) the average number of itinerant d electrons in the alloy, being proportional to

$N_{FeFe,g}/N_{Fe,n}$. The exact dependence cannot be deduced at present, but in order that the formula should contain the first case above, the product must be given the exponent $\frac{1}{2}$.

It should be emphasized that the interpretation of H_{eff} given here need not be unique. It is reasonably clear that we have observed a preferred exchange interaction of s electrons with Fe-Fe bonds rather than with Fe-Sn bonds. We propose that this can be ascribed to anisotropy of the spin polarization, but we have not excluded possible other causes for such a preference.

B. Solid Solutions FeSn

In applying Eq. (3), it must be remembered that the factor $(N_{FeFe,g}/N_{Fe,n})^{1/2}$ contains the ratio of $3d$ electrons that are of a collective (itinerant) nature. In dilute solid solutions FeSn, we assume that all $3d$ electrons are partaking in the band and we choose $(N_{FeFe,g}/N_{FeFe,n}) = 1$. This gives

$$H_{eff,FeSn}(Fe) = 8^{-1/2} H_{eff,iron}(Fe) N_{Fe'Fe}^{1/2}, \quad (4)$$

where $H_{eff,iron}(Fe)$ is the magnetic hf field in iron metal. This should be compared with the equation used by Wertheim *et al.*⁹ and by Stearns¹⁰ for dilute solutions:

$$H_{eff,FeSn}(Fe) = H_{eff,iron}(Fe) \times (1 - N_{Fe'Sn} h_1 - N'_{Fe'Sn} h_2 - \dots), \quad (5)$$

where h_1 and h_2 are effects caused by one nearest and one next-nearest neighbor, respectively, N and N' are the numbers of nearest and next-nearest neighbors, and the indices have the same meaning as above. A small concentration-dependent factor has been omitted in Eq. (5). Effects of second-nearest neighbors were computed by Wertheim *et al.*,⁹ while Stearns¹⁰ has given numerical results for surrounding atoms up to the fifth-nearest neighbor. In the present work, we consider only the effects of nearest neighbors.

Our experimental values for tin contents 4 and 8 at.%, are plotted in Fig. 1, together with the numbers obtained by using Eq. (4). In Eq. (5), our data for FeSn give $h_1 = (6.0 \pm 1.0)\%$ to be compared with the value $(7.3 \pm 0.5)\%$ of Ref. 9. Values^{9,10} of h_1 for eight other elements dissolved in iron lie in the region 6.5–8.3%, while FeCo appears as an exception (4.3%).

Equation (5) is based on the assumption that the s -electron spin density at the iron nucleus can be added up as a sum of separate contributions from each single neighbor impurity. However, Eq. (4), being based on a different approach, is also in agreement with experiment, since it can be written

$$H_{eff,FeSn}(Fe) = 8^{-1/2} H_{eff,iron}(Fe) (8 - N_{Fe'Sn})^{1/2} = H_{eff,iron}(Fe) (1 - 0.0625 N_{Fe'Sn})^{1/2}$$

$$\times -0.00195 N_{\text{Fe}'\text{Sn}}^2 + \dots). \quad (6)$$

By comparison with (5), h_1 attains the values 6.45, 6.64, and 6.83%, corresponding to 1, 2, and 3 Sn nearest neighbors, respectively. The measurements are not sufficiently precise to show whether h_1 may have variations of this magnitude. One must conclude that neither the experiments nor the theory are sufficiently developed to show whether the spin densities in these solid solutions are additive.

C. Other Structures

The application of Eq. (3) to ferromagnetic intermetallic compounds is straightforward and gives a fairly good fit, as shown in Fig. 1. The equation was also applied to two antiferromagnetic structures with iron atoms ordered ferromagnetically in planes (FeSn) and in rows (FeSn₂). For FeSn, the equation reproduces $H_{\text{eff}}(\text{Fe})$ very well, although the magnetic moment per Fe atom is only 77% of its value in iron. For FeSn₂, the equation gives the right value if we assume that all 3d electrons take part in Fe-Fe bonding, i. e., the calculation must be done as if there are no tin neighbors, $N_{\text{Fe}'\text{Sn}} = 0$. The Fe-Sn distance is, in fact, fairly long, 2.8 Å. This particular application of Eq. (3) is probably rather extreme.

In order to test the possible general validity of Eq. (3), we have applied it to the bcc structure Fe₃X for which Stearns²³ has obtained values of $H_{\text{eff}}(\text{Fe})$ in the cases of X=Si and Al. In this lattice $N_{\text{Fe},n} = 8$, but iron has two different positions site A with $N_{\text{Fe}'\text{Fe}}(A) = 4$ and site D with $N_{\text{Fe}'\text{Fe}}(D) = 8$. For the quantity $N_{\text{Fe}'\text{Fe},g}$, we used the average value $5\frac{1}{3}$. Table VII shows a comparison between the values of Stearns and our calculation. The somewhat low values obtained by the calculation may indicate that Si and Al produce less disturbance in the Fe lattice ferromagnetism than do the larger Sn atoms. It should be noted that these hf fields are also roughly proportional to the magnetic moments. Therefore, these results do not indicate whether one or the other principle is correct.

Mössbauer-effect studies on Fe₃Ge and Fe₅Ge₃ were performed by Yamamoto.²⁶ Fe₃Ge has two modifications: a cubic LI₂ structure with $|H_{\text{eff}}(\text{Fe})| = (271 \pm 5)$ kG and a hexagonal DO₁₉ structure with

$|H_{\text{eff}}(\text{Fe})| = (268 \pm 5)$ kG. We recall that Fe₃Sn has DO₁₉ structure, with $H_{\text{eff}}(\text{Fe}) = (-268 \pm 2)$ kG. The coordination numbers are equal in these two structures, so that Eq. (3) gives -277 kG for all three cases. The most accurate Mössbauer study of Fe₅Ge₃ was performed by Germagnoli *et al.*,²⁷ who found that the magnetic hf field is strongly composition dependent. This structure is quite similar, or equal, to Fe₅Sn₃. The Mössbauer spectra have roughly the same appearance in the two cases, both containing a couple of poorly resolved components with $H_{\text{eff}}(\text{Fe})$ between 195 and 255 kG. Again, these examples lend some support to the assumption that magnetic hf fields are predominantly determined by coordination numbers.

V. MAGNETIC MOMENTS

Neutron diffuse-scattering experiments by Holden, Comly, and Low²⁸ show that the tin atoms in FeSn carry no, or only a very small, magnetic moment. The additional fact that the average moment per iron atom, $\bar{\mu}_{\text{Fe}}$, is roughly constant for all ferromagnetic Fe-Sn compounds can be taken to indicate that $\mu_{\text{Sn}} \approx 0$ in all Fe-Sn alloys.

For the solid solutions, the magnitude of $\bar{\mu}_{\text{Fe}}$ increases linearly with tin content by $0.17 \mu_B/\text{Fe}$ atom, corresponding to addition of 8 at % of tin. The same tendency has been obtained by Aldred,⁸ who also observes a similar increase for antimony in iron, a smaller increase for gold, gallium, germanium, and arsenic, while some lighter solute atoms obey a dilution model, as they appear to be purely nonmagnetic holes in the structure. The increase in iron moment caused by heavy nontransition solute atoms can either be ascribed to an increase in the 3d moment or to a decrease in a small negative 4s moment. Some evidence for a negative 4s polarization is provided by neutron-diffraction measurements²⁹ and by polarized-positron annihilation.³⁰ These experiments indicate that the atomic moment of iron metal, $2.2 \mu_B$, would be composed by about $2.4 \mu_B$ from the 3d electrons, and about $-0.2 \mu_B$ caused by the 4s electrons. The latter contribution could partly disappear as the conduction electrons are being used for Fe-Sn bonding.

A net conduction-electron polarization (CEP) in iron metal can be caused by two different effects: (i) exchange coupling between *d* and *s* electrons, causing "attraction" between equal spins, and giving a polarization in the direction of magnetization; (ii) covalent mixing between *s* and *d* wave functions, giving negative *s* polarization because the covalent mixing is dominating among electrons of minority spin. On the whole, theoretical estimates concerning the sign of the net CEP in iron are inconclusive.^{25,31}

If variations in the magnetic moment of FeSn are

TABLE VII. Ratios of magnetic hf fields in alloy sites A and D to the value in iron metal.

	Expt results		Calculated from Eq. (3)
	by Stearns (Ref. 23)		
	Fe ₃ Si	Fe ₃ Al	
$H_{\text{eff}}(A)/H_{\text{eff, iron}}(\text{Fe})$	0.60	0.64	0.58
$H_{\text{eff}}(D)/H_{\text{eff, iron}}(\text{Fe})$	0.94	0.89	0.82

caused mainly by changes of CEP, this could imply a $3d$ polarization which is largely constant and unchanged by alloying, as described by Friedel's rigid-band model. The fact that $\bar{\mu}_{\text{Fe}}$ is roughly equal for Fe, Fe_3Sn , Fe_5Sn_3 , and Fe_3Sn_2 lends support to this interpretation. The small linear increase in $\bar{\mu}_{\text{Fe}}$ caused by large atoms (Sn, Sb) in solution and not by small ones (Si, Al) may be explained by noting that the smaller atoms are more electronegative, so that the screening takes place on the solute atom itself.³² The iron bonding to the small atoms is, therefore, more ionic and causes less depolarization than the covalentlike bonding between iron and tin.

Arajs, Chessin, and Dunmyre³³ have observed an exceptionally high increase in electrical resistivity when tin is added to iron. This indicates a vanishing conduction band and supports the above interpretation.

It is interesting to note that this model for the magnetic moment of metallic iron with tin impurities implies that the hf field $H_{\text{eff}}(\text{Fe})$ is rather insensitive to changes in the conduction band. Experimental values for magnetic moment and hf field are given in Figs. 1 and 3 and in Table I. For $N_{\text{Fe}, \text{Fe}} = 8$ and 7, the value of $H_{\text{eff}}(\text{Fe})$ varies by less than 2% while the magnetic moment per Fe atom increases about 9% as tin is dissolved in iron. One can also find a couple of other physical facts which indicate that $H_{\text{eff}}(\text{Fe})$ may not be very sensitive to changes in CEP. It was shown above that measurements on dilute solid solutions of a number of different metals in iron give a coefficient h_1 which is rather independent of the type of solute. One might expect the different charge contrasts to have different effects upon the conduction-electron distribution. Any such variation in the conduction band has apparently little influence upon the hf field. Freeman and Watson²² have reviewed some other hf data which indicate the same conclusion. In particular, it appears that for an iron atom in a transition-metal host the field at the nucleus is given predominantly by its own electrons, and it is largely independent of the surroundings.

On the other hand, there exist several results which show that CEP may contribute considerably to the magnitude of $H_{\text{eff}}(\text{Fe})$. Stearns¹⁰ has performed a very detailed analysis of Mössbauer-effect data from a number of FeX alloys. The obtained oscillations in the hf field as a function of impurity distance are similar to the conduction-electron spin-density variations of the type described by the RKKY theory. The predicted variations are many times smaller than the observed ones, but this could be ascribed to the approximate nature of the theory. In their review on H_{eff} at solute atoms in ferromagnets, Shirley, Rosenblum, and Matthias³⁴ estimate the value $H_{\text{CEP}} = -120$ kG for

iron dissolved in iron. Exchange-polarized Hartree-Fock calculations²¹ show that one spin-up $4s$ electron in an iron ion would contribute 1850 kG to the hf field. This result is valid for s electrons in closed shells, and in principle it is inapplicable to electrons in an unfilled band, but it shows clearly that CEP may give a very large contribution to H_{eff} .

Although there are many data concerning these problems, they are not at present sufficient to form a clear picture. One must conclude that the important question regarding the effect of CEP upon the hf and magnetic moment of ferromagnetic iron has not been answered yet.

VI. MAGNETIC hf FIELD AT TIN NUCLEI

The magnetic field at Sn nuclei in iron-tin alloys are varying more strongly than the magnetic moments of the Fe atoms. Actually, the ratio $H_{\text{eff}}(\text{Sn})/\bar{\mu}_{\text{Fe}}$ has values between 0 and 45 kG/ μ_B . When this ratio is plotted against the number of nearest-neighbor iron atoms, as in Fig. 2, the ferromagnetic compounds appear to follow roughly a proportionality law

$$H_{\text{eff}}(\text{Sn}) = H_2 N_{\text{SnFe}, \uparrow} \bar{\mu}_{\text{Fe}}, \quad (7)$$

where $N_{\text{SnFe}, \uparrow}$ is the number of spin-up nearest neighbors minus the number of spin-down nearest neighbors. The straight dashed line in Fig. 2 corresponds to the coefficient $H_2 = 3.8$ kG/ μ_B . Tin atoms in the ferromagnetic planes of the antiferromagnetic FeSn have a value somewhat above the straight line. For FeSn_2 there is no preferred orientation of the neighbors' spins. Even if one assumes preferred bonding directions, choosing $N_{\text{SnFe}, \uparrow} = 2$, the experimental value is much higher than expected.

By comparing fields obtained from free-atom hf structure with observed values for the magnetic fields at the nuclei of various impurities dissolved in iron, Shirley and Westenbarger³⁴ found an approximate proportionality between the two sets of data. This indicates that the transferred hf field is caused mainly by CEP. A systematic study³⁴ of magnetic hf fields on solute atoms in a ferromagnetic host indicates that CEP is an important part of the origin of these fields. However, for tin, being a $5p$ metal, this effect may be comparatively small. A couple of different mechanisms can be imagined as contributing to the spin distribution of the solute conduction electrons. For instance, one would expect open $3d$ shells to exchange polarize conduction electrons on neighboring atoms. Daniel and Friedel³⁵ have shown that the spin distribution at the nucleus of nontransition elements dissolved in iron can be obtained from the sum of the free electron and the "bound-conduction-electron" contributions. The theory gives satisfactory agreement with experiment for elements up to xenon. It

implies, however, that high valencies, for instance, valency 8 for xenon, have to be acknowledged.³⁶ Shirley³⁷ has shown that in these solutions the exchange interaction would give a too small effect, and the Daniel-Friedel theory is a too rough approximation at high valency of the solute. The most important contribution to spin distribution of the 5s electrons in tin atoms would rather be caused by overlap with the orbits of the polarized 3d electrons of the neighboring iron atoms.

As shown in Sec. V, our own data indicate that conduction electrons are unimportant for the magnitude of $H_{\text{eff}}(\text{Fe})$ in the solid solutions FeSn. This is compatible with the idea that the transfer of hf fields is not a pure conduction-electron effect, but rather is caused by *d-s* orbital overlap. Such a mechanism could even be responsible for transferred hf fields in all the Fe-Sn compounds. In that case the observed additivity of contributions from nearest-neighbor iron atoms would be easy to understand. In the tin-rich compounds FeSn and FeSn₂, the 3d electron orbits are apparently strongly localized since the additivity law is not valid in these cases.

VII. ISOMER SHIFTS

The isomer shift δ for Mössbauer spectra on Fe and Sn are given in Table I and plotted in Fig. 6. The values are relative to metallic iron and white tin, respectively, so that in the expression³⁸

$$\delta = \frac{4}{3}\pi Ze^2R^2S'(Z)(\Delta R/R) [|\psi(0)|_{\text{abs}}^2 - |\psi(0)|_{\text{source}}^2] \quad (8)$$

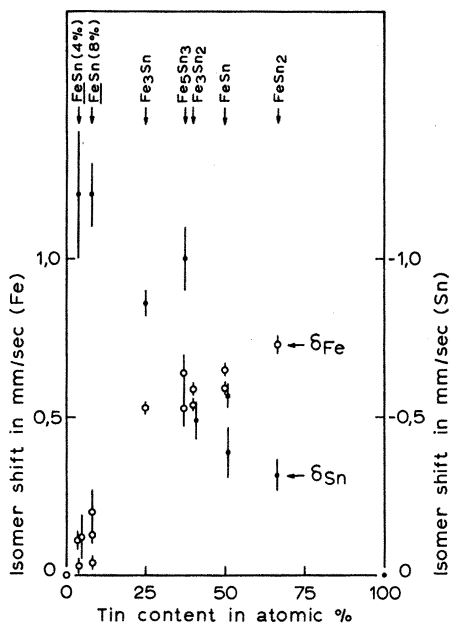


FIG. 6. Isomer shifts in iron-tin alloys at Fe (circles) and at Sn (black dots) positions, relative to iron metal and white tin, respectively.

the electron density $|\psi(0)|_{\text{source}}^2$ must be considered as the value in the pure metal. Here, Z is atomic number, R is the nuclear radius, $S'(Z)$ is a "relativity factor," and $\Delta R/R$ is the relative increase on excitation of the nucleus. We adopt the ratio $\Delta R/R = -1.8 \times 10^{-3}$ for the 14-keV transition in iron and $\Delta R/R = 1.2 \times 10^{-4}$ for the 24-keV transition in tin.³⁹ When these quantities are introduced in Eq. (8) together with the observed data given in Table I, it is seen that the electron densities at the nuclear sites are *reduced* at all nuclei in Fe-Sn alloys with respect to the densities in the pure metals. Figure 6 shows that the isomer shifts approach the iron/white tin metal value, as the compound content of iron/tin is increased.

If it is assumed that the isomer shifts are primarily caused by localized bonds made up of the valence electrons of iron and tin, then every bond could be expected to contribute equally to the isomer shifts, and the contributions would be additive. When the alloy is given as Fe_xSn_y, one might expect the ratio $x\delta_{\text{Fe}}/y\delta_{\text{Sn}}$ to be a constant, independent of composition. In Table VIII and in Fig. 7(a) the experimental values of this ratio are given. It varies between 0.73 and 1.81, but the constant order of magnitude shows that there is a connection between concentration and isomer shift.

The systematic trend of the isomer shifts is more clearly exhibited by taking into consideration the actual coordination numbers of the different compounds. Therefore, the ratio of isomer shift to the number of Fe-Sn bonds δ_i/N_{ij} has been calculated for the structures which are reasonably well known. The values for this ratio should be the same for all alloys, provided that all Fe-Sn bonds were constructed in exactly the same way. Experimental results are given in Table VIII and are plotted in Figs. 7(b) and (c). For completeness, Qaim's measurement⁴⁰ on iron as an impurity in tin, yielding $\delta_{\text{Fe}} = -0.395 \pm 0.020$ mm/sec has been included. The ratios obtained have, indeed, approximately a constant value, both for iron and for tin. We note that the solid solution values for δ_{Sn} appear not to follow the general trend. However, one might assume that also second-nearest neighbors in the bcc lattice can influence the isomer shift. This would give $N_{\text{SnFe}} = 14$ instead of 8, and the two left-hand points in Fig. 7(c) would drop to the value 0.086 mm/sec, in good agreement with the other alloys. Horizontal dashed lines in Fig. 7 correspond to chosen average values, which can be used to formulate two general isomer-shift relations:

$$\delta_{\text{Fe}} = \delta'_{\text{Fe}} N_{\text{FeSn}} = 0.105 N_{\text{FeSn}} \text{ mm/sec}, \quad (9)$$

$$\delta_{\text{Sn}} = \delta'_{\text{Sn}} N_{\text{SnFe}} = -0.09 N_{\text{SnFe}} \text{ mm/sec}. \quad (10)$$

These equations are necessarily of a very approxi-

TABLE VIII. Isomer shift systematics for Fe-Sn alloys.

Fe_xSn_y	$\frac{x}{y} \frac{\delta_{Fe}}{\delta_{Sn}}$	N_{FeSn}	N_{SnFe}	$\frac{\delta_{Fe}}{N_{FeSn}}$	$\frac{\delta_{Sn}}{N_{SnFe}}$
<i>FeSn</i> (1 nn Sn)					
4 % Sn ($x/y=8$)	-0.73 ± 0.30	1	8	0.11 ± 0.03	-0.15 ± 0.03
8 % Sn ($x/y=8$)	-0.87 ± 0.25	1	8	0.13 ± 0.03	-0.15 ± 0.01
Fe_3Sn	-1.85 ± 0.11	4	12	0.132 ± 0.005	-0.072 ± 0.004
$Fe_5Sn_3^a$	-1.00 ± 0.15	5.6(av)	9.3(av)	0.107 ± 0.010	-0.107 ± 0.011
$Fe_3Sn_2^a$	-1.74 ± 0.23				
$FeSn^a$	-1.23 ± 0.20	6	6	0.105 ± 0.004	-0.085 ± 0.010
$FeSn_2$	-1.15 ± 0.18	8	4	0.091 ± 0.004	-0.080 ± 0.013
$FeSn(1 \text{ nn Fe})^b$		4-6		0.10-0.07	

^aValue used is a weighted average.

^bData by S. M. Qaim (Ref. 40).

mate nature. Many effects that can influence the isomer shift have been disregarded. It must, for instance, be expected that the distances between the atoms in the compound are of considerable importance.

It should also be noted that the alloys with tin content below 38 at. % apparently belong to a group with high isomer shift, $\delta_{Sn} \approx -1.0$ mm/sec. A similar result⁴¹ has been obtained for SnCu alloys, where $\delta_{Sn} \approx -1.0$ mm/sec for tin content below 15 at. %. This apparent saturation magnitude of the isomer shift corresponds to the value obtained in chemical compositions where tin has tetravalent bonds with a small ionic character.⁴² The four nearest neighbors are then bound to tin by hybridized (sp^3) covalent bonds. The results for the al-

loys, therefore, indicate that all the tin valence electrons can take part in the metallic covalentlike bonding, and this would happen when there is a sufficient number of nearest neighbors of the other element. The necessary coordination number could be $N_{Sn,x} \geq 8$, implying that the delocalized metallic bonds oscillate (resonate) between two sets of four neighbors. This condition is indeed satisfied for the alloys in question: *FeSn*, Fe_3Sn , and Fe_5Sn_3 .

A coarse calculation of the changes in electron densities at the nuclear sites can be performed by use of Eq. (8) and the data given by Shirley.³⁸ From his Fig. 1, we get the approximate values

$$|\psi_{4s}(0)|^2 = 0.11 \times 10^{26} \text{ cm}^{-3} \quad \text{for Fe,}$$

$$|\psi_{5s}(0)|^2 = 1.20 \times 10^{26} \text{ cm}^{-3} \quad \text{for Sn.}$$

$S'(Z)$ is tabulated in Ref. 38, and we assume that there is one 4s electron in Fe and one 5s electron in Sn. The ratios $\Delta R/R$ are given above, and for R the value of $1.2A^{1/3} \times 10^{-13}$ cm is used. By means of these data and the average experimental values for δ' as given in Eqs. (9) and (10), we get the following rough numerical estimate: Every Fe-Sn bond influences the electron densities at the nuclei by amounts corresponding to removal of about 0.08 s electron from the iron atom and about 0.03 s electron from the tin atom.

This trend is expected as a natural consequence of the fact that electrons in pure single-lattice metals are excluded by the Pauli principle from overlap in the region between atomic cores. In an alloy no such restriction would exist for electrons situated between atoms of different elements. Thus, the s-electron densities at the nuclei in the alloy can be reduced with respect to the pure metals. Qualitatively, the observed isomer shifts therefore show the cancellation of the exclusion effect, caused by iron-tin bonding.

In addition, it must be remembered that the s-electron densities at iron nuclei can be influenced strongly by d-electron screening.⁴³ Similarly, from Wilson's⁴⁴ Hartree-Fock calculations of the screening effects on $|\psi_{5s}(0)|^2$, it is seen that the effect of

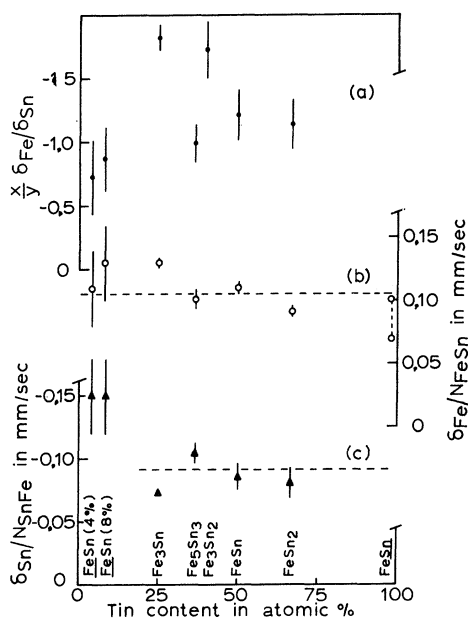


FIG. 7. Different representations of isomer-shift data for iron-tin alloys. (a) Isomer-shift ratio times composition ratio, (b) Fe isomer shift divided by Sn coordination, (c) Sn isomer shift divided by Fe coordination.

adding one $5p$ electron to a $5s^25p^2$ configuration in tin corresponds roughly to the removal of one-sixth of a $5s$ electron. The Fe-Sn bond will probably not influence the d -electron population, but a change in the $5p$ -electron density is very possible.

VIII. CONCLUSION

Any complete theory describing the electronic and magnetic properties of iron-tin alloys must be able to account for the following experimental facts:

(i) $\bar{\mu}_{Fe}$ is nearly equal for all the ferromagnetic phases Fe, Fe_3Sn , Fe_5Sn_3 , and Fe_3Sn_2 . (ii) $\bar{\mu}_{Fe}$ is increasing linearly as tin is added to iron in solid solution. (iii) $H_{eff}(Fe)$ is proportional to $\bar{\mu}_{Fe}$ for tin contents above 37 at. % but not for the iron-rich alloys. A more general rule, such as Eq. (3), which includes the atomic coordinations is necessary to describe $H_{eff}(Fe)$. (iv) $H_{eff}(Sn)$ is not proportional to $\bar{\mu}_{Fe}$. Rather, Eq. (7), which includes coordinations, seems to be valid for ferromagnetic alloys. (v) Isomer shifts in these compounds show that the s -electron densities at both iron and tin nuclei are reduced in proportion to the number of Fe-Sn bonds.

These data, taken together with other observations, suggest the following explanation: The $4s$ electrons in metallic iron are negatively polarized by about $0.2\mu_B$ per atom, with respect to the $3d$ electrons. The conduction band is partly destroyed when tin is dissolved in iron, and the conductivity is reduced. The negative-spin $4s$ electrons are partly depolarized and the magnetic moment per iron atom is increasing. This implies that changes in the net spin of the conduction electrons in dilute iron alloys have a small effect upon the magnitude of $H_{eff}(Fe)$, which therefore stays constant in a given coordination. It should be noted that there is also some evidence showing that a considerable part of $H_{eff}(Fe)$ in iron metal may be caused by CEP, and it is difficult to combine our interpretation with that one. When more tin is added, and intermetallic compounds are formed, the $3d$ net spin stays approximately constant as long as the alloy is ferromagnetic. The bond formation influ-

ences the spatial distribution of the $3d$ spin, which has a strong effect upon core polarization. Hence, $H_{eff}(Fe)$ will vary considerably with the structure. The results suggest that the exchange interaction responsible for Fe core polarization is caused primarily by electrons in the Fe-Fe bonds, while the $3d$ electrons situated between iron and tin atoms are localized and less important for the polarized d - s exchange interaction.

The transferred hf field $H_{eff}(Sn)$ is caused primarily by $3d$ - $5s$ orbital overlap. The Fe-Sn bond is of an unsaturated covalentlike nature (metallic bond, consisting of sp^3 hybrids) in which the electrons are largely unpolarized. The valence s electrons have a higher density in the region between atoms than is the case for pure metals.

Regardless of this qualitative interpretation, we believe that the systematic trends (i)-(v) above and the empirical equations (3), (7), (9), and (10) can give useful information on the electron structure and the exchange interaction in these alloys. It would be very valuable if similar effects could be observed in other alloy systems. There does already exist some data which indicate that Eq. (3) may have a more general validity for nontransition elements alloyed with iron.

A number of properties of particular Fe-Sn compounds were observed in the course of this work. Some of these are (i) the magnetic order in the phases Fe_3Sn , Fe_5Sn_3 , and Fe_3Sn_2 is pure ferro- and not ferrimagnetism. (ii) In Fe_3Sn , the magnetic moment is directed along the c axis. (iii) Fe_5Sn_3 can exist in one phase with the vacancies in the Fe II planes statistically distributed, and in another phase with the Fe II atoms ordered in a yet unknown structure, having a lattice unit $4a$. (iv) Fe_3Sn_2 has a phase transition at $114^\circ K$. This transition point is raised in an external magnetic field. (v) In $FeSn$, the magnetic moment of one-third of the Fe atoms is directed along the major EFG axis, and two-thirds are directed at 60° to this axis. (vi) In $FeSn_2$, the electron distribution has less symmetry than the geometrical structure, since $Fe\uparrow - Sn - Fe\uparrow$ bonding appears to be favored.

¹M. Hansen and K. Anderko, *Constitution of Binary Alloys* (McGraw-Hill, New York, 1958), p. 718.

²C. Jannin, P. Lecocq, and A. Michel, *Compt. Rend.* **257**, 1906 (1963).

³K. Yamaguchi and H. Watanabe, *J. Phys. Soc. Japan* **22**, 1210 (1967).

⁴C. Djéga-Mariadassou (unpublished).

⁵W. Nicholson and E. Friedmann, *Bull. Am. Phys. Soc.* **8**, 43 (1963).

⁶J. B. Goodenough, *Magnetism and the Chemical Bond* (Interscience, New York, 1963).

⁷M. Fallot, *Ann. Phys. (Paris)* **6**, 305 (1936).

⁸A. T. Aldred, *J. Phys. C* **1**, 1103 (1968).

⁹G. K. Wertheim, V. Jaccarino, J. H. Wernick, and

D. N. E. Buchanan, *Phys. Rev. Letters* **12**, 24 (1964).

¹⁰M. B. Stearns, *Phys. Rev.* **147**, 439 (1966).

¹¹A. J. F. Boyle, D. S. P. Bunbury, and C. Edwards, *Phys. Rev. Letters* **5**, 553 (1960).

¹²O. Nial, *Svensk Kem. Tidskr.* **59**, 165 (1947).

¹³C. Djéga-Mariadassou, P. Lecocq, E. Both, and G. Trumpy (unpublished).

¹⁴H. Yamamoto, *J. Phys. Soc. Japan* **21**, 1058 (1966).

¹⁵C. Djéga-Mariadassou, P. Lecocq, G. Trumpy, J. Träff, and P. Østergård, *Nuovo Cimento* **46**, 35 (1967).

¹⁶C. Djéga-Mariadassou, P. Lecocq, and A. Michel, *Ann. Chim. Phys.* **4**, 175 (1969).

¹⁷P. Iyengar, B. Dasnamacharya, R. R. Vijayaraghavan, and A. P. Roy, *J. Phys. Soc. Japan* **17**, 1947 (1962).

- ¹⁸V. I. Nikolaev, Yu. I. Shcherbina, and A. I. Karchevskii, *Zh. Eksperim, i Teor. Fiz.* **44**, 775 (1963)[Soviet Phys. JETP **17**, 524 (1963)]; V. I. Nikolaev, Yu. I. Shcherbina, and S. S. Yakimov, *ibid.* **45**, 1277 (1963) [*ibid.* **18**, 878 (1964)].
- ¹⁹G. Fabri, E. Germagnoli, M. Musci, and G. C. Locati, *Nuovo Cimento* **40B**, 178 (1965).
- ²⁰R. E. Watson and A. J. Freeman, in *Hyperfine Interactions*, edited by A. J. Freeman and R. B. Frankel (Academic, New York, 1967), p. 53.
- ²¹R. E. Watson and A. J. Freeman, *Phys. Rev.* **123**, 2027 (1961).
- ²²A. J. Freeman and R. E. Watson, in *Magnetism*, edited by G. T. Rado and H. Suhl (Academic, New York, 1965), Vol. II A, p. 167.
- ²³M. B. Stearns, *Phys. Rev.* **168**, 588 (1968).
- ²⁴G. Shirane, C. W. Chen, P. A. Flinn, and R. Nathans, *Phys. Rev.* **131**, 183 (1963).
- ²⁵C. Herring, in *Magnetism*, edited by G. T. Rado and H. Suhl (Academic, New York, 1966), Vol. IV.
- ²⁶H. Yamamoto, *J. Phys. Soc. Japan* **20**, 2166 (1965).
- ²⁷E. Germagnoli, C. Lamborizio, S. Mora, and I. Ortalli, *Nuovo Cimento* **42B**, 314 (1966).
- ²⁸T. M. Holden, J. B. Comly, and G. G. Low, *Proc. Phys. Soc. (London)* **92**, 726 (1967).
- ²⁹C. G. Shull and Y. Yamada, *J. Phys. Soc. Japan* **17**, 1 (1962).
- ³⁰P. E. Mijnarends and L. Hambro, *Phys. Letters* **10**, 272 (1964).
- ³¹W. E. Mott, *Advan. Phys.* **13**, 325 (1964).
- ³²J. Friedel, *Nuovo Cimento Suppl.* **7**, 287 (1958).
- ³³S. Arajs, H. Chessin, and G. R. Dunmyre, *J. Appl. Phys.* **36**, 1370 (1965).
- ³⁴D. A. Shirley and G. A. Westenbarger, *Phys. Rev.* **138**, A170 (1965); D. A. Shirley, S. S. Rosenblum, and E. Matthias, *ibid.* **170**, 363 (1968).
- ³⁵E. Daniel and J. Friedel, *J. Phys. Chem. Solids* **24**, 1601 (1963).
- ³⁶L. Niesen, J. Lubbers, H. Postma, H. de Waard, and S. A. Drentje, *Phys. Letters* **24B**, 144 (1967).
- ³⁷D. A. Shirley, *Phys. Letters* **25A**, 129 (1967).
- ³⁸D. A. Shirley, *Rev. Mod. Phys.* **36**, 339 (1964).
- ³⁹H. Wegener, *Der Mössbauereffekt und seine Anwendung in Physik und Chemie* (Bibliographisches Institut, Mannheim, Germany, 1966).
- ⁴⁰S. M. Qaim, *Proc. Phys. Soc. (London)* **90**, 1065 (1967).
- ⁴¹V. V. Chekin and V. G. Naumov, *Zh. Eksperim, i Teor. Fiz.* **50**, 534 (1966)[Soviet Phys. JETP **23**, 355 (1966)].
- ⁴²V. I. Goldanskii, *At. Energy Rev.* **1**, 3 (1963).
- ⁴³L. R. Walker, G. K. Wertheim, and V. Jaccarino, *Phys. Rev. Letters* **6**, 98 (1961).
- ⁴⁴M. Wilson, *Phys. Rev.* **176**, 58 (1968).

Mössbauer-Effect Study of Europium in Glass

M. F. Taragin and J. C. Eisenstein

Department of Physics, The George Washington University, Washington, D. C. 20037

(Received 11 June 1970)

Mössbauer spectra have been obtained for ¹⁵¹Eu in some silicate and phosphate glasses. In the silicate glasses Eu³⁺ behaves very much as it does in Eu₂O₃. The isomer shift relative to Eu₂O₃ is ~0.1 mm/sec. Some broadening of the line can be attributed to unresolved quadrupole splitting and to disorder in the glass structure. The recoilless fraction is 0.33. Measurements made at elevated temperatures indicate a complicated dependence of isomer shift on temperature cycling. In europium phosphate glass the isomer shift is ~-0.3 mm/sec, and the linewidth is approximately the same as for the silicate glasses.

INTRODUCTION

Approximately ten papers have been published¹ about the Mössbauer effect of iron in various alkali silicate, borosilicate, borate, and phosphate glasses. There have also been a number of studies² of tin in glass. Thus far, however, only two papers have dealt with the Mössbauer effect of rare-earth ions in glass, and both of these³ were about Tm³⁺. Because of the technological importance of glasses doped with rare-earth ions, it is worthwhile to exploit any experimental technique which yields information about their structure. It is well known that Mössbauer spectra yield information about the ionization or valence state of the Mössbauer ion, the site symmetry, and the local electric and magnetic

fields. Still other information can sometimes be obtained, for example, by varying the temperature of the specimen. This paper deals with the Mössbauer spectra of several silicate glasses which contain different amounts of Eu₂O₃, and with europium phosphate glass.

SAMPLES

All of our samples were obtained from Cleek of the Inorganic Glass Section of the National Bureau of Standards. The analysis of the silicate glasses is given in Table I. The phosphate glass was made by mixing stoichiometric amounts of europium oxide and ammonium phosphate and heating. The resulting glass presumably has the composition Eu(PO₃)₃. The absorbers were prepared by grinding the